Targeted Delivery of a Triplex-Forming Oligonucleotide to Hepatic Stellate Cells†

Zhaoyang Ye,‡ Kun Cheng,‡ Ramareddy V. Guntaka,*,§ and Ram I. Mahato*,‡

Departments of Pharmaceutical and Molecular Sciences, University of Tennessee Health Science Center, Memphis, Tennessee 38163

Received November 23, 2004; Revised Manuscript Received January 13, 2005

ABSTRACT: Liver fibrosis is characterized by abnormal accumulation of extracellular matrix (ECM), namely, fibrillar collagens in the hepatic stellate cells (HSCs). Earlier, we developed an antigene approach, using a type α1(I) collagen gene promoter specific triplex-forming oligonucleotide (TFO) to inhibit collagen gene expression. In this paper, to enhance overall delivery of TFOs to the liver and more specifically to HSCs, we synthesized mannose 6-phosphate-bovine serum albumin (M6P-BSA) by phosphorylating *p*-nitrophenyl-α-D-mannopyranoside, reducing its nitro group, and reacting it with thiophosgene to produce *p*-isothiocyanatophenyl-6-phospho-α-D-mannopyranoside (itcM6P) for conjugation with BSA. ^{33}P-TFO was conjugated with M6P-BSA via a disulfide bond, and the stability of the $(M6P)_{20}$-BSA-TFO conjugate was determined. Following tail vein injection into rats, $(M6P)_{20}$-BSA-^{33}P-TFO rapidly cleared from the circulation and accumulated mainly in the liver. Almost 66% of the injected $(M6P)_{20}$-BSA-^{33}P-TFO accumulated in the liver at 30 min postinjection, which was significantly higher than that deposited after injection of ^{33}P-TFO. A large proportion of the injected $(M6P)_{20}$-BSA-^{33}P-TFO was taken up by the HSCs as evidenced by determination of radioactivity in the digested liver cells upon liver perfusion and separation on a Nycodenz gradient. Therefore, this TFO conjugate may be used for the treatment of liver fibrosis.

Fibrosis of almost all organs in the body leads to organ dysfunction and is a major health problem. Fibrosis is characterized by an excessive production of extracellular matrix (ECM) components, predominantly type I and III fibrillar collagens found in various tissues (*1*, *2*). We developed a triplex-forming oligonucleotide (TFO),[1] which can form a triplex with the target sequence (C1) located in the α1 (I) collagen gene promoter (*3*−*5*). In the liver, hepatic stellate cells (HSCs) are the principle cell type responsible for abnormal production of collagens (*6*, *7*). Therefore, if we can specifically inhibit transcription of type I collagen gene in HSCs, we should be able to prevent liver fibrosis.

Following systemic administration, oligonucleotides (ODNs) widely distribute throughout the body with higher uptake in the liver and kidney (*8*−*10*). To date, there are several reports on targeted delivery of ODNs to hepatocytes, Kupffer cells, and liver endothelial cells (*11*, *12*), but no information is available on ODN delivery to HSCs, which comprises only 5−15% of all the liver cells (*13*). The mannose 6-phosphate/insulin like growth factor II (M6P/IGF II) receptor is expressed on HSCs, and its expression is up-regulated upon activation of these cells due to acute or chronic liver injury (*14*, *15*). Beljaars et al. (*16*) demonstrated a preferential distribution of M6P conjugated human serum albumin (HSA) to HSCs after systemic administration into rats. Bonfils et al. (*17*) conjugated 19mer ODNs to M6P-BSA via disulfide bond and demonstrated 2-fold higher cellular uptake by macrophages (J774 cells) as compared to fibroblast-like BHK cells and 30-fold higher than monocytes (U937 cells). However, these authors did not determine the biodistribution and uptake of the M6P-BSA-ODN conjugate by different liver cells.

To maximize TFO delivery to the liver in general and to HSCs in particular, we synthesized M6P-BSA and conjugated it to TFO via a disulfide bond. TFOs were labeled with ^{33}P prior to conjugation with M6P-BSA, and the stability and biodistribution of the $(M6P)_{20}$-BSA-^{33}P-TFO conjugate was determined after tail vein injection into rats. Intrahepatic cellular distribution was also determined by collagenase liver perfusion at 30 min after intravenous injection of $(M6P)_{20}$-BSA-^{33}P-TFO followed by fractionation on a Nycodenz gradient.

MATERIALS AND METHODS

Materials. Bovine serum albumin (BSA) (fraction V, purity >98%) was purchased from USB Corporation (Cleveland, OH). *p*-Nitrophenyl-α-D-mannopyranoside (pnpM), phosphorus oxide chloride, palladium (10 wt % on activated carbon), thiophosgene, bromophenol blue, 0.04% trypan blue, dithiothreitol (DTT), and Pronase were purchased from Sigma-Aldrich Chemicals Limited (St. Louis, MO). *N*-

† This work was supported by Grant RO1 DK064633 from the NIH and USPHS Grant 47379.

* Corresponding authors. (R.I.M.) Tel: (901) 448-6929; fax: (901) 448-6092; e-mail: rmahato@utmem.edu. (R.V.G.) Tel: (901) 448-8230; fax: (901) 448-8462; e-mail: rguntaka@utmem.edu.

‡ Department of Pharmaceutical Science.

§ Department of Molecular Science.

[1] Abbreviations: APS, antiparallel phosphorothioate; BCA, bicinchonic acid; BSA, bovine serum albumin; DTT, dithiothreitol; ESI−MS, electrospray ionization−mass spectrometry; Gal-PLL, galactosylated poly(L-lysine); HSCs, hepatic stellate cells; itcM6P, *p*-isothiocyanatophenyl-6-phospho-α-D-mannopyranoside; M6P, mannose 6-phosphate; ODNs, oligodeoxynucleotides; PAGE, polyacrylamide gel electrophoresis; papM6P, *p*-aminophenyl-6-phospho-α-D-mannopyranoside; pnpM, *p*-nitrophenyl-α-D-mannopyranoside; SPDP, *N*-succinimidyl 3-(2-pyridyldithio)-propionate; Sulfo-LC-SPDP, sulfosuccinimidyl 6-[3′-(pyridyldithio)-propionamido]-hexanoate; TFO, triplex-forming oligonucleotide.

10.1021/bi047529j CCC: $30.25
Published on Web 02/25/2005

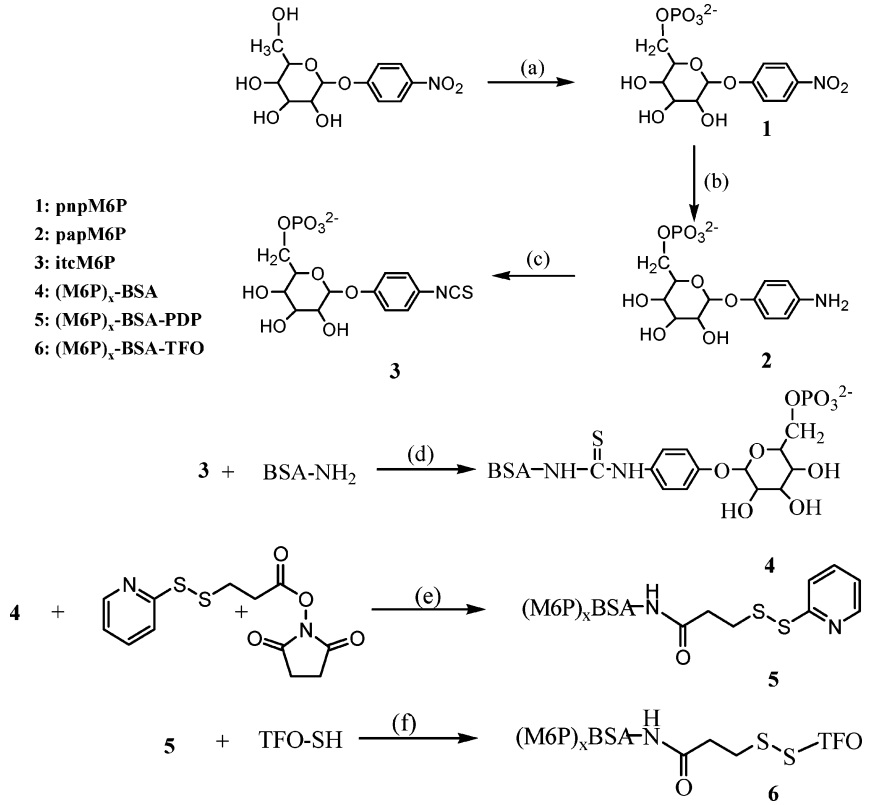

FIGURE 1: Synthesis of M6P-BSA-TFO. *x* stands for the number of M6P residues per BSA molecule. Reagents and conditions: (a) $POCl_3$, acetonitrile, pyridine, H_2O; (b) 10% Pd/C, 1 atm H_2, ethanol/H_2O (v/v: 4/1); (c) thiophosgene, chloroform, 0.1 M sodium carbonate buffer, pH 8.6; (d) 0.1 M sodium carbonate buffer, pH 9, 0.15 M NaCl; (e) 0.1 M sodium borate buffer, pH 8.6, ethanol; and (f) (1) 0.2 M DTT, 0.1 M glycine buffer containing 0.1 M NaCl, pH 9.0 and (2) 0.1 M glycine buffer containing 0.1 M NaCl, pH 9.0.

Succinimidyl 3-(2-pyridyldithio)-propionate (SPDP) and a bicinchonic acid (BCA) protein assay kit were purchased from Pierce (Rockford, IL). PD-10 desalting columns and Sephadex G75 (superfine) were obtained from Pharmacia Fine Chemicals AB (Uppsala, Sweden). Dialysis tubing (molecular weight cutoff of 3500 Da) was purchased form Spectrum Laboratories. Inc. (Houston, TX). BioGel P-6 DG gel was from Bio-Rad Laboratories (Hercules, CA). [γ-^{33}P]-dATP was purchased from MP Biomedicals (Irvine, CA), and T4 polynucleotide kinase was from New England Biolabs (Beverly, MA). Soluene-350 (tissue solubilizer) and HionicFluor (scintillation fluid) were purchased from Perkin-Elmer (Boston, MA). Hydrogen peroxide (H_2O_2) was purchased from Fisher Chemical (Fair Lawn, NJ). Heparin was purchased from American Pharmaceutical Partners, Inc. (Los Angeles, CA). Ca^{2+}/Mg^{2+}-free Hank's balanced salt solution (Cellgro) was purchased from Media Tech (Washington, DC), and type IV collagenase was from Worthington Biochemical Corporation (Lakewood, NJ). Isoflurane was purchased form Baxter Pharmaceutical Products, Inc. (Deerfield, IL). Nycodenz AG was purchased from Greiner Bio-One, Inc. (Longwood, FL). All solvents and other chemicals used in this study were used as purchased without further treatment.

ODNs (Figure 2) for the target C_1 region (−170 to approximately −141) of the α1 (I) collagen gene promoter, T1 (30mer, 5′-CCT TTC CCT TCC TTT CCC TCC TCC CCC CTC-3′) and T2 (30mer, 5′-GAG GGG GGA GGA GGG AAA GGA AGG GAA AGG-3′), and TFO, which was a 25mer antiparallel fully phosphothioate ODN (3′-GAG GGG GGA GGA GGG AAA GGA AGG G-5′), were

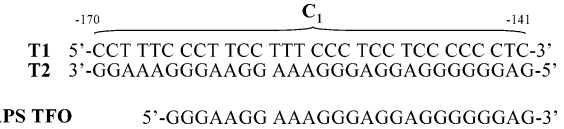

FIGURE 2: Sequences of ODNs, T_1, and T_2, for target duplex C_1 region (−170 to −141) of the rat α1 (I) collagen promoter and triplex-forming oligonucleotide (TFO). Phosphorothioate oligonucleotide used for triplex formation in antiparallel orientation (APS TFO) is shown aligned with corresponding target regions (from −165 to −141).

synthesized by The Midland Certified Reagent Company, Inc. (Midland, TX), or the same TFO modified with a sulfhydryl group at the 3′ end (MW: 8684.0 Da) was synthesized by Invitrogen Life Technologies (Carlsbad, CA).

Animals. Male Sprague−Dawley rats weighing 150−170 g were purchased from Harlan Co. (San Diego, CA) and were housed individually under the controlled light (12/12 h) and temperature conditions and had free access to food and water.

Synthesis of p-Isothiocyanatophenyl-6-phospho-α-D-mannopyranoside. *p*-Nitrophenyl-α-D-mannopyranoside (pnpM) was phosphorylated (Figure 1, step a) at the 6 position reacting with phosphorus oxide chloride as described by Roche et al. (*18*) (Figure 1). Briefly, pnpM (0.3 g, 1 mmol) was dissolved in pyridine (0.4 mL, 5 mmol), acetonitrile (1 mL, 19 mmol), and water (0.04 mL, 2.2 mmol). Phosphorus oxide chloride (0.4 mL, 4.4 mmol) was added, and the mixture was stirred for 1 h on an ice−water bath. The reaction mixture was poured onto 20 g of ice. After the ice melted, the pH was adjusted to 7.0 by slowly adding 2.5 M NaOH, and the solution was evaporated to dryness. The solid

material was dissolved in 25 mL of water, and the solution was concentrated to a final volume of 2−3 mL under reduced pressure at 35 °C. The concentrated solution was kept at 4 °C overnight for crystallization, and crystals were filtered and washed with 5 mL of absolute ethanol. The compound was recrystallized in a mixture of 1 mL of water and 10 mL of ethanol, redissolved in water, and lyophilized to give *p*-nitrophenyl-6-phospho-α-D-mannopyranoside (pnpM6P) (0.25 g). The product was characterized using ^{1}H NMR and mass spectrometry. For ^{1}H NMR, the samples were dissolved in D_2O, and the spectra were recorded on a Bruker ARX-300 MHz NMR spectrometer (Bruker, Billerica, MA) at 25 °C. For electrospray ionization (ESI) mass spectrometry, samples were dissolved in a mixture of methanol/H_2O (v/v: 4/1), and spectra were recorded on an ESQUIRE-LC Ion Trap LC/MS(n) system (Bruker, Billerica, MA).

PnpM6P (**1**) (0.25 g, 0.66 mmol) was reduced with 100 mg of 10% palladium on activated carbon under H_2 (1 atm) in 20 mL of a 4:1 (v/v) methanol−water mixture for 2 h (Figure 1, step b) as described by Monsigny et al. (*19*). After filtration, the solvent was evaporated under reduced pressure. The residue was redissolved in water and lyophilized to give *p*-aminophenyl-6-phospho-α-D-mannopyranoside (papM6P) (compound **2**, Figure 1).

Thiophosgene (55 μL, 0.73 mmol) in 10 mL of chloroform was added to papM6P (**2**) (50 mg, 0.14 mmol) in 10 mL of 0.1 M sodium carbonate buffer, pH 8.6, and the mixture was vigorously stirred for 1 h as described by Sando and Karson (*20*). Chloroform was then removed, and the aqueous phase was extracted several times with 10 mL of chloroform to remove unreacted thiophosgene and lyophilized to give *p*-isothiocyanatophenyl-6-phospho-α-D-mannopyranoside (itcM6P) (compound **3**, Figure 1).

Synthesis of M6P-BSA. M6P-BSA was synthesized as described by Sando and Karson (*20*) by 26 to 75 mg of itcM6P being dissolved in 2.0 mL of 0.1 M sodium carbonate buffer, pH 9, and 0.15 M NaCl, and then 30 mg (0.45 μmol) of BSA slowly was added in 2.0 mL of the same buffer. The reaction mixture was kept at room temperature for 18 h with stirring and then applied to a PD-10 column, previously equilibrated with 0.1 M sodium phosphate buffer (0.15 M NaCl, pH 6.0). Fractions (between 2.5 and 6 mL) that contained the M6P-BSA conjugate were dialyzed extensively in sodium phosphate buffer at 4 °C for 2 to 3 days, freeze-dried, and stored at −20 °C. By the molar ratio of BSA and itcM6P being varied, with concentrations of up to 96 μmol/mL itcM6P and 15 mg/mL BSA, we obtained M6P-BSA with a different number of M6P residues. The conjugates were verified on an 8% sodium dodecyl sulfate−polyacrylamide gel electrophoresis (SDS−PAGE).

Synthesis of M6P-BSA-PDP. To have activated disulfide bonds for conjugation with TFOs, 20 mg of BSA or M6P-BSA was dissolved in 1 mL of 0.1 M sodium borate buffer, pH 8.6, and *N*-succinimidyl 3-(2-pyridyldithio)-propionate (SPDP) (4 mg, 12.8 μmol) in 0.65 mL of ethanol, and the mixture was stirred for 20 h at room temperature (*21*). The products were purified on a PD-10 column by elution with PBS and then with H_2O/1-butanol (95:5, v/v) and then freeze-dried. The number of PDP groups coupled to M6P-BSA or BSA was determined from absorbance at 343 nm in the presence of DTT as described by Carlsson et al. (*22*). BSA concentration in each sample was determined by BCA protein assay kit using the vendor's protocol. The conjugate formation was also confirmed on 8% SDS−PAGE. Mercaptoethanol was not added in the loading buffer to prevent dissociation of disulfide bonds in PDP groups.

Determination of Sugar Content. Sugar content was determined by the resorcinol-sulfuric acid method as described by Monsigny et al. (*23*). Two hundred microliters of 6 mg/mL resorcinol and 1 mL of 75% sulfuric acid was added to the sample containing 5−100 nmol of sugars in a volume of 200 μL. The mixtures were shaken by vortex and heated at 90 °C for 30 min and subsequently placed in a cold-water bath for 30 min in the dark. The optical density of the solution was measured at 430 nm. PnpM was used to generate the standard curve determining the sugar concentrations.

Labeling of TFOs. TFO was labeled by adding γ-^{33}P to the 5′ end terminal using [γ-^{33}P]dATP and T4 polynucleotide kinase using the manufacturer's protocol. Briefly, 1 μg of TFO was mixed with 8 μL of buffer containing 2 μL of [γ-^{33}P]dATP and 1 μL of T4 polynucleotide kinase (25 units). The reaction mixture was incubated at 37 °C for 45 min, stopped when the sample was heated to 70 °C for 10 min, and was diluted to a final volume of 100 μL. Unincorporated [γ-^{33}P]dATP was removed from the labeled TFOs by size-exclusion chromatography with BioGel P-6 DG gel. The incorporation efficiency of the purified ^{33}P-TFO was measured by a TCA precipitation method, and the value was more than 95%. The specific activity (cpm/μg) of the ^{33}P-TFO was about $5-10 \times 10^7$ cpm/μg. Radioactivity was measured on a TRI-CARB 2000 liquid scintillation analyzer (PACKARD Instrument Company, Meriden, CT).

Synthesis of M6P-BSA-TFO. TFO modified with a sulfhydryl group at the 3′ end (115 nmol) and mixed with 0.115 nmol of ^{33}P-TFO ($\sim 5 \times 10^7$ cpm/μg) was treated with 0.2 M DTT in 300 μL of 0.1 M, pH 9.0, glycine buffer containing 0.1 M NaCl for 3 h at room temperature to generate a 3′-thiol functional group. Excess DTT was removed by extraction with ethyl acetate (4 × 400 μL), and TFO was precipitated by adding 2.6 vol of ethanol after the addition of NaOAc to 0.3 M. The mixture was placed at −20 °C overnight and centrifuged for 30 min at 13 000*g*. The TFO pellet was dissolved in 600 μL of deionized water, and 2.5 mg of $(M6P)_{20}$-BSA-PDP in 200 μL of deionized water was added followed by addition of 100 μL of the glycine buffer. The mixture was incubated with stirring at room temperature for 24 h. The product was eluted with PBS on a G 75 column (1 × 25 cm). Fractions (0.5 mL each) containing protein were collected, freeze-dried, and stored at −80 °C. Radioactivity and TFO concentration of each fraction were determined using a scintillation counter and a BioMate 3 spectrophotometer (Thermo Spectronic, Rochester, NY), respectively. The formation of the $(BSA)_{20}$-M6P-TFO conjugate was verified by electrophoresis on a 20% native polyacryamide gel at room temperature.

Triplex Formation. TFO was heated at 65 °C for 10 min to prevent self-aggregation and then quickly quenched on ice. The duplex was prepared by equal amounts of ODNs, T1: 5′-GAG GGG GGA GGA GGG AAA GGA AGG GAA AGG-3′ and T2: 5′-CCT TTC CCT TCC TTT CCC TCC TCC CCC CTC-3′ in Figure 2, being heated at 80 °C for 5 min in 0.25 M NaCl, followed by slow cooling to room temperature. Triplex formation was initiated by the mixing

of 3 μL of 3 × buffer [135 mM Tris-acetate, pH 7.0, 30 mM $MgCl_2$], 3.5 μL of duplex DNA (~3 ng), and 2.5 μL of the $(M6P)_{20}$-BSA-^{33}P-TFO conjugate (~7×10^4 cpm). The reaction mixture was incubated at 37 °C for 6 h. Two microliters of a 50% glycerol solution containing bromophenol blue was added, and samples were directly loaded onto 15% native polyacrylamide gel, prepared in a buffer containing 50 mM Tris-acetate, pH 7.0, and 10 mM $MgCl_2$. Electrophoresis was performed at 8 V/cm at 4 °C in the buffer containing 89 mM Tris-Borate and 20 mM $MgCl_2$. The gel was autoradiographed at 4 °C overnight.

In Vitro Stability of M6P-BSA-TFO. The stability of the M6P-BSA-^{33}P-TFO conjugate was checked in the presence of rat serum. Four microliters of $(BSA)_{20}$-M6P-^{33}P-TFO in 0.9% saline (~10^5 cpm) was incubated with 6 μL of rat serum for 1, 2, 4, and 6 h at 37 °C. After incubation, the samples were applied on 20% native PAGE at room temperature at 8 V/cm for 60 min. ^{33}P-TFO was used as a control. The gel was autoradiographed at 4 °C overnight to determine the stability of $(M6P)_{20}$-BSA-^{33}P-TFO.

Biodistribution of $(M6P)_{20}$-BSA-^{33}P-TFO. The protocol of animal use and care was approved by the Comparative Department of the University of Tennessee Health Science Center. Male Sprague−Dawley rats weighing 150 to ~170 g were anesthetized by inhalation of isoflurane, and then 250 μL of ^{33}P-TFO or $(M6P)_{20}$-BSA-^{33}P-TFO in saline (~2.2×10^5 cpm) was injected intravenously into Sprague−Dawley rats at a dose of 0.2 mg of TFO/kg body weight. After a set time, blood (0.2−0.3 mL) was collected by cardiac puncture in heparinized tubes, and urine was also collected directly from the urinary bladder using a 26-gauge needle syringe. Major organs, such as liver, spleen, kidney, lung, heart, and muscle, were isolated, washed with saline, blotted dry, weighed, and stored at −86 °C. Blood was centrifuged, and plasma was separated. One hundred and fifty microliters of plasma or 150−200 g of each tissue was incubated with 2 mL of solubilizer Soluene-350 for 3 h at 55 °C first and then overnight at room temperature. Two hundred microliters of 30% H_2O_2 was added to each sample and incubated for another 30 min. Ten milliliters of HionicFluor scintillation fluid was added to each tissue, plasma, and urine sample, and the radioactivity of each sample was measured using a scintillation counter.

Isolated Rat Liver Perfusion. To determine the effect of M6P on the hepatic uptake of TFOs by parenchymal cells (hepatocytes) and nonparenchymal cells (Kupffer, endothelial, and Stellate cells), the liver was perfused in situ after intravenous administration of ^{33}P-TFO or $(M6P)_{20}$-BSA-^{33}P-TFO at the dose of 0.2 mg of TFO/kg body weight (*10*, *24*). At 30 min post-administration, rats (300−350 g) were anesthetized by inhalation of isoflurane, 100 U heparin was injected via the tail vein, the abdomen was opened, and the portal vein was cannulated with PE-60 polyethylene tube. The liver was first perfused with 2 mL of diluted heparin solution at 20 units/mL to avoid blood clogs in the liver. The liver was preperfused in situ with 200 mL of Ca^{2+}/Mg^{2+}-free Hank's balanced salt solution at a flow rate of 15 mL/min and was then perfused with Hank's balanced salt solution containing 0.05% type IV collagenase and 0.1% Pronase for additional 250 mL at a flow rate of 10 mL/min. All the perfusion solutions were incubated at 37 °C.

After perfusion, the liver was removed to Hank's balanced salt solution, and all the extraneous tissue was cut away without damaging the capsule. The capsule was disturbed with forceps, and the cells were freed into the medium by a fair amount of agitation of the forceps in the medium. The suspension was passed through a sterilized gauze. The cell suspension was centrifuged at 50*g* for 5 min, the pellet containing hepatocytes was resuspended in Hank's buffer, and viability was determined by tryptan blue staining. The supernatant was enriched in nonparenchymal cells and was further centrifuged at 100*g* for 5 min to remove residual parenchymal cells. Nonparenchymal cells were collected by centrifugation of the supernatant at 500*g* for 10 min. HSCs were further separated from Kupffer and endothelial cells using the gradient method as described by Hendriks et al. (*25*). To generate a gradient, collected nonparenchymal cells were dispersed in 10 mL of Nycodenz solution at 11.5%. Under part of the gradient, 5 mL of 17.5% Nycodenz solution was layered, and these two solutions were overlayed with 2 mL of PBS. This gradient was then spun at 1450*g* for 17 min with a slow acceleration and deceleration. After centrifugation, the top of the second layer (11.5%) contained purified HSCs, and the top of the 17.2% layer contained Kupffer and endothelial cells. Separated cells were counted. 10×10^6 of each cell type was digested with Soluene-350 overnight. Hionic-Fluor was added, and the radioactivity was counted using a liquid scintillation counter. The contributions of various cell types to the total liver uptake were calculated as described previously (*26*) and expressed as ng of TFO per mg of cell protein.

Statistical Analysis. Data were expressed as the mean ± standard deviation (SD). $P < 0.05$ was considered statistically significant. Statistics were calculated based on an unpaired student's *t*-test or the Behrens-Fisher test using SAS software.

RESULTS

To enhance the hepatic uptake of TFOs, we synthesized M6P-BSA and conjugated it to TFO via disulfide bond formation. M6P-BSA-TFO conjugates were then characterized in terms of stability, whole body, and intrahepatic distribution.

Synthesis and Characterization of M6P-BSA and M6P-BSA-PDP. The synthesis scheme of M6P-BSA conjugates carrying different numbers of M6P residues is shown in Figure 1. *P*-Nitrophenyl-α-D-mannopyranoside (pnpM) was phosphorylated to give *p*-nitrophenyl-6-phospho-α-D-mannopyranoside (pnpM6P). ESI−MS and ^{1}H NMR results of this intermediate product are as follows: ESI−MS (negative-ion mode): 379.8 ($[M + H]^-$); ^{1}H NMR (D_2O): δ 8.15 (d, 2H), 7.16 (d, 2H), 5.65 (s, 1H), 3.56−4.06 (m, 6H). PnpM6P was reduced to *p*-aminophenyl-6-phospho-α-D-mannopyranoside (papM6P) with ESI−MS (negative-ion mode): 350.1 ($[M + H]^-$) and ^{1}H NMR (D_2O): δ 6.93 (d, 2H), 6.71 (d, 2H), 5.34 (s, 1H), 3.67−4.04 (m, 6H). PapM6P was reacted with thiophosgene to produce isothiocyanatophenyl-6-phospho-α-D-mannopyranoside (itcM6P), with the following ESI−MS and ^{1}H NMR spectra: ESI−MS (negative-ion mode): 392.0 ($[M + H]^-$); ^{1}H NMR (D_2O): δ 7.18 (d, 2H), 7.05 (d, 2H), 5.50 (s, 1H), 3.56−4.02 (m, 6H) (Figure 3). Three M6P-BSA derivatives, $(M6P)_{11}$-BSA, $(M6P)_{21}$-BSA, and $(M6P)_{34}$-BSA, were synthesized by the starting ratio of

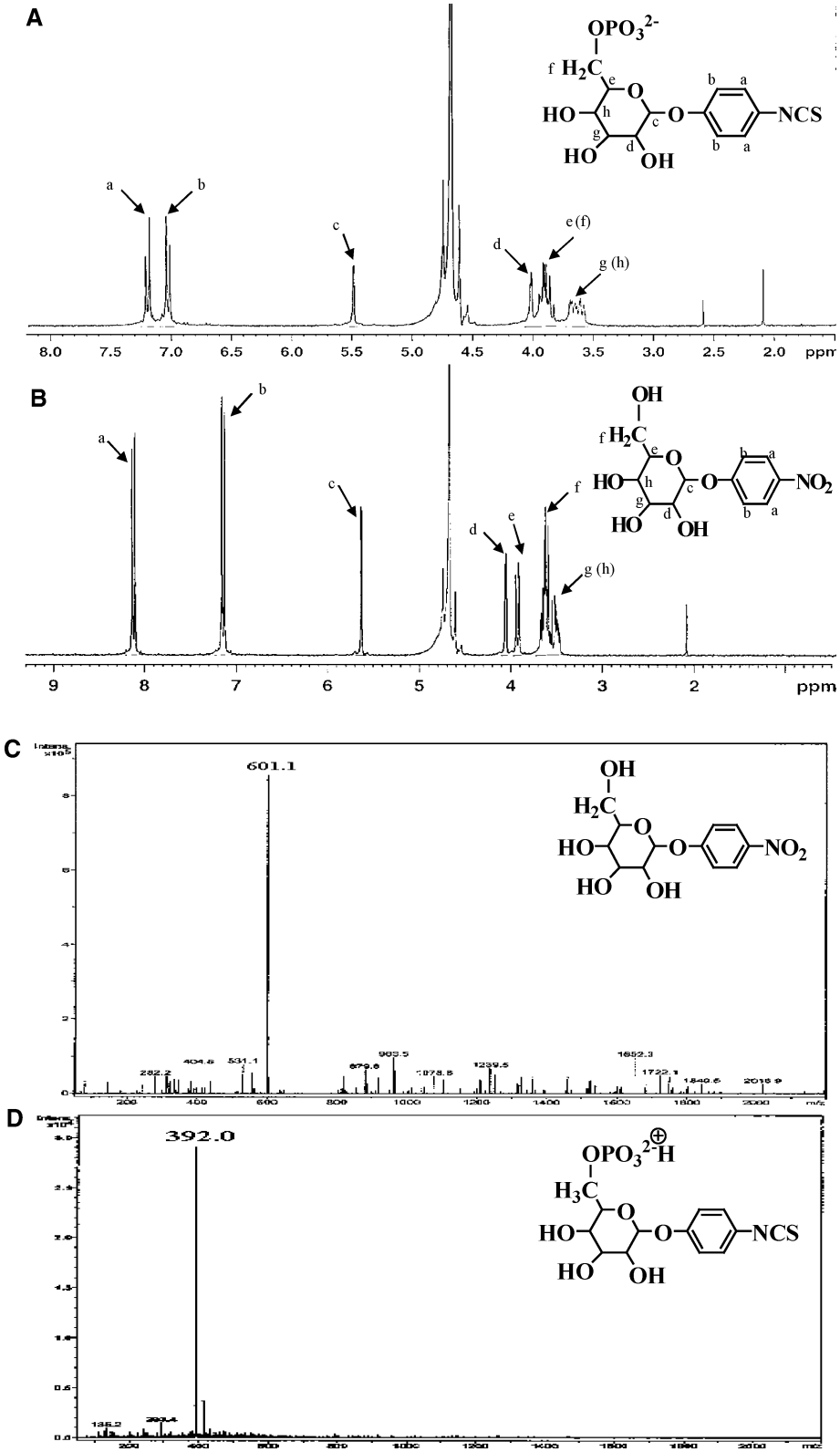

FIGURE 3: Characterization of intermediate products with ^{1}H NMR and ESI−MS. For ^{1}H NMR, samples were dissolved in D_2O, and the spectra were recorded on a Bruker ARX-300 MHz NMR spectrometer at 25 °C. Electrospray ionization (ESI) mass spectra were obtained in a mixture of methanol/H_2O (v/v: 4:1) on an ESQUIRE-LC Ion Trap LC/MS(n) system. (A and B) ^{1}H NMR spectra of ictM6P and pnpM. (C and D) ESI−MS spectra of pnpM and itcM6P.

itcM6P to BSA being changed from 180 to 425, and these BSA derivatives contained 11, 21, and 34 of M6P residues, respectively (Table 1). The PDP groups were then conjugated to BSA and M6P-BSA derivatives to introduce activated disulfide bonds for conjugation with TFOs, which were modified with sulfhydryl groups at the 3′ ends. In $(M6P)_8$-BSA-PDP, BSA-PDP-1, and BSA-PDP-2, there were around 15 PDP groups. However, there were only ∼6 PDP groups in $(M6P)_{20}$-BSA-PDP and $(M6P)_{27}$-BSA-PDP because BSA had already been conjugated with a higher number of M6P

Table 1: Determination of M6P and PDP Contents of BSA Derivatives

BSA derivatives	PDP content[a] (mol/mol BSA)	sugar content[b] (mol/mol BSA)
PDP-BSA-1	14.7	0
PDP-BSA-2	15.7	0
$(M6P)_{11}$-BSA	0	11.0
$(M6P)_{21}$-BSA	0	21.2
$(M6P)_{34}$-BSA	0	34.0
$(M6P)_8$-BSA-PDP	15.6	7.6
$(M6P)_{20}$-BSA-PDP	6.7	19.7
$(M6P)_{27}$-BSA-PDP	6.0	27.1

[a] The PDP content was determined as described by Carlsson et al. (*22*). [b] Sugar content was determined by resorcinol/sulfuric acid method (*23*).

groups as compared to $(M6P)_8$-BSA-PDP, which also utilized amine groups in BSA. These derivatives were confirmed on the 8% SDS−PAGE by band retardation (Figure 4). The bands of BSA derivatives on the gel were retarded as compared to those of BSA indicating the formation of different conjugates and an increase in the molecular weights of these derivatives after conjugation. The bands in lanes 6−9 were not clear possibly due to conjugation of a large number (i.e., 34) of M6P residues and/or PDP residues that might have affected Commassie blue staining of proteins. Therefore, we also determined the protein contents in these samples by BCA assay. Zhang et al. had reported similar phenomenon when these authors stained M6P-HSA before and after conjugation with glycyrrhetin (*27*).

Synthesis and Characterization of M6P-BSA-TFO. M6P-BSA was conjugated to the TFO by disulfide bond formation between PDP groups of M6P-BSA and the TFOs, which were modified with sulfhydryl group at the 3′ end. The conjugate was purified on a Sephadex G 75 column (1× 25 cm), and a typical elution profile is shown in Figure 5. Unreacted TFO was separated from the conjugate very well. We used 1 × PBS containing 0.5 M NaCl to elute the conjugate. In contrast, when only PBS was used as an elution buffer, the separation was very bad because we used phosphorothioate TFO, which is known to bind serum easily (*8*). However, at high salt concentration (0.5 M NaCl), binding efficiency of TFO to BSA was significantly decreased. The TFO and BSA contents in each fraction were determined, and the molar ratio of TFO and BSA in each fraction was calculated and plotted in Figure 5B. From fractions 8−17, approximately one TFO molecule was attached to one BSA molecule, and after that the ratios of TFO and BSA were suddenly increased to higher than 2 (fraction 18), which meant that the free TFO was eluted out. Thus, fractions from 8−17 were combined, freeze-dried, and stored at −80°C for future use.

Stability of M6P-BSA-^{33}P-TFO. The disulfide bond of the M6P-BSA-TFO conjugate is expected to be stable in the plasma, and TFO should not be released unless the conjugate is taken up by the cells. Conjugation of M6P-BSA to TFO via a disulfide bond formation was confirmed on a 20% native PAGE (Figure 6). In the absence of DTT, the $(M6P)_{20}$-BSA-^{33}P-TFO conjugate stayed on the top of the gel because of its large molecular weight. There were two bands both in lane 3 and in lane 4. The upper bands in lanes 3 and 4 were multimers of $(M6P)_{20}$-BSA-^{33}P-TFO, and the lower bands were its monomer form. The same phenomenon was noticed by Bonfils et al. (*17*). The multimer is the cluster of several molecules of monomer $(M6P)_{20}$-BSA-^{33}P-TFO associated together, so it has a very high molecular weight. We confirmed this by treating the conjugate with Proteinase K, in which the whole sample was digested to release TFO (Figure 8, lane 4). When treated with DTT (Figure 8, lanes 5 and 6), the bands corresponding to $(M6P)_{20}$-BSA-^{33}P-TFO conjugate disappeared, and a new band in the much lower part of the gel appeared, which corresponded to free TFO molecules. However, there was also a faint band in lanes 5 and 6, which is likely to be the G-quartet structure of the TFO molecules since there is a 6-guanine sequence in the TFO we used (Figure 2), which is easy to form a G-quartet structure. (*28*) We have shown that the G-quartet structure could be efficiently removed by the sample being heated in a boiling water bath for 10 min and then cooled in an ice bath (K. Cheng et al., manuscript in preparation), and this was also confirmed by the results shown in Figure 8, lane 4, in which the sample was heat-treated to remove the G-quartet structure, and there was no quartet structure.

To determine its stability, the $(M6P)_{20}$-BSA-^{33}P-TFO conjugate was incubated with rat serum at 37 °C for 6 h. As shown in Figure 7, there were no other bands in the gel except those two bands corresponding to the multimer and monomer of the $(M6P)_{20}$-BSA-^{33}P-TFO conjugate, which stayed on the top of the 20% polyacrylamide gel. These results suggest that the disulfide bond between TFO and M6P-BSA as well as the ^{33}P labeling were stable in serum at least up to 6 h.

Effect of M6P-BSA on Triplex Formation. Disulfide linkage between TFO and M6P-BSA is expected to be stable in the bloodstream but will be cleaved inside the cells by disulfide exchange with intracellular thiols or by the action of redox enzymes (*29*). The release from the M6P-BSA-TFO conjugate will enable TFO to traffic to the nucleus for triplex formation with genomic DNA. There should be no adverse effect on triplex formation due to this conjugation and cleavage. The $(M6P)_{20}$-BSA-^{33}P-TFO conjugate was treated with DTT and incubated with the target duplex DNA

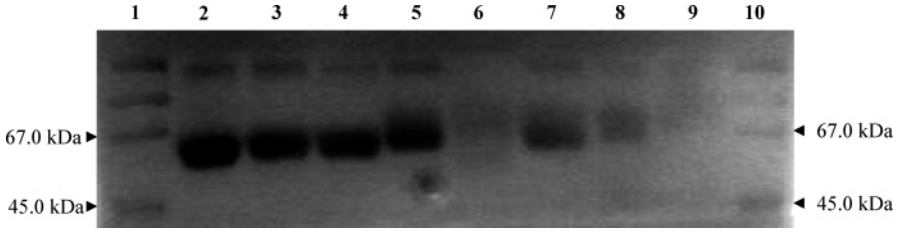

FIGURE 4: SDS−PAGE (8%) of BSA and BSA derivatives. Electrophoresis was performed under 8 v/cm at room temperature for 3 h in 1× TBE buffer. Gel was stained with Commassie brilliant blue. Lane 1: protein standard marker; lane 2: BSA; lane 3: BSA-PDP-1; lane 4: BSA-PDP-2; lane 5: $(M6P)_{11}$-BSA; lane 6: $(M6P)_{34}$-BSA; lane 7: $(M6P)_8$-BSA-PDP; lane 8: $(M6P)_{20}$-BSA-PDP; lane 9: $(M6P)_{27}$-BSA-PDP; and lane 10: prestained SDS−PAGE protein standard marker.

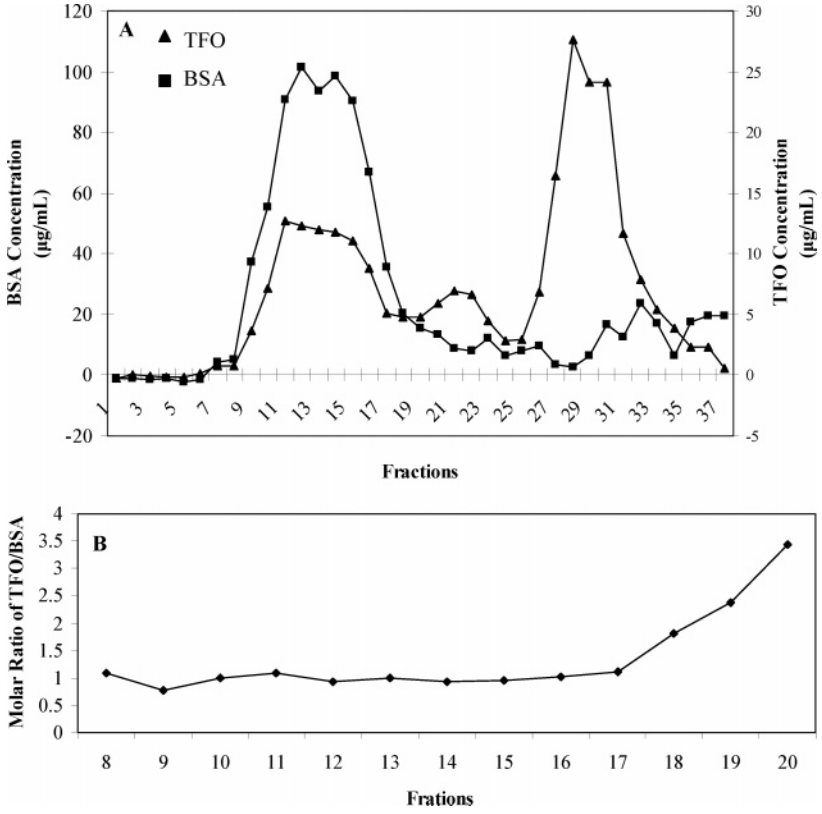

FIGURE 5: (A) Purification of M6P-BSA-TFO conjugate using gel chromatography. The reaction mixture was eluted with 1× PBS buffer containing 0.5 M NaCl on a Sephadex G75 column. (B) Molar ratios of TFO/BSA in different fractions.

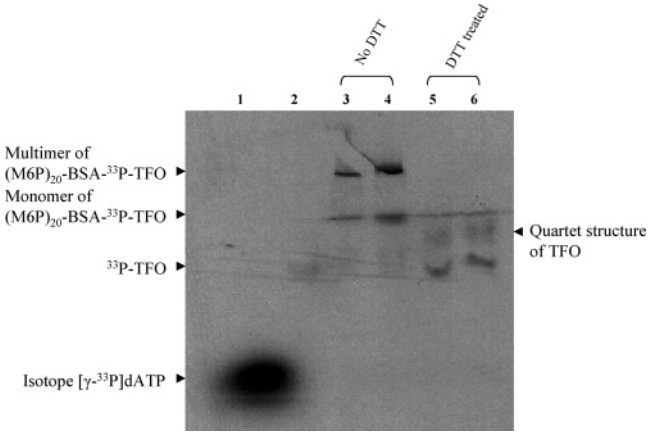

FIGURE 6: Formation of disulfide bond between M6P-BSA-PDP and TFO. Electrophoresis was performed on a 20% native PAGE at 8 V/cm for 2 h at room temperature in 1× TBE buffer. The gel was autoradiographed at 4 °C overnight. Lane 1: free isotope [γ-^{33}P]dATP; lane 2: ^{33}P-TFO; lane 3: $(M6P)_{20}$-BSA-^{33}P-TFO (2 μl); lane 4: $(M6P)_{20}$-BSA-^{33}P-TFO (3 μL); lane 5: $(M6P)_{20}$-BSA-^{33}P-TFO (2 μL) + DTT (1 mg); and lane 6: $(M6P)_{20}$-BSA-^{33}P-TFO (3 μL) + DTT (1.5 mg).

for 6 h, and the sample was then applied on a 15% native polyacrylamide gel at 4 °C. Following electrophoresis, the gel was autoradiographed at 4 °C overnight. As shown in Figure 8, there was triplex formation between free TFO and target duplex DNA (lane 3), which was at a molar ratio of 500 between duplex DNA and TFO. However, in the case of the $(M6P)_{20}$-BSA-^{33}P-TFO conjugate, the ratio of TFO to duplex DNA used was 2, and with this much lower ratio, a portion of released TFO still formed a triplex with the target duplex DNA, which is shown when lanes 6 and 7 are compared.

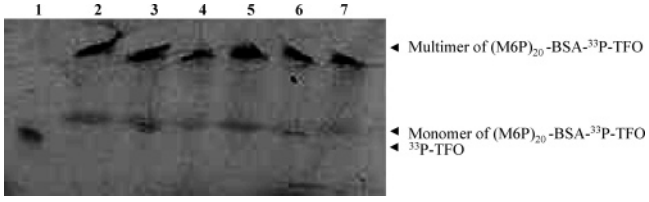

FIGURE 7: Stability of M6P-BSA-TFO in rat serum. Four microliters of $(M6P)_{20}$-BSA-^{33}P-TFO ($\sim$1 × 10^5 cpm) was incubated with 6 μL of rat serum at 37 °C for a defined period and then applied to 20% PAGE. The electrophoresis was performed under 8 V/cm at room temperature. Lane 1: ^{33}P-TFO; lane 2: 0 h; lane 3: 0.5 h; lane 4: 1 h; lane 5: 2 h; lane 6: 4 h; and lane 7: 6 h.

Biodistribution of M6P-BSA-TFO Conjugate. Following synthesis and purification of M6P-BSA and then conjugation to ^{33}P-TFO, we determined the biodistribution of $(M6P)_{20}$-BSA-^{33}P-TFO and ^{33}P-TFO at 5 and 30 min postinjection into the rat tail vein. Figure 9 shows the time course of radioactivity in the plasma, urine, liver, kidney, lung, heart, and muscle. In the case of ^{33}P-TFO, almost 40% of the injected dose was detected in the plasma at 5 min postinjection but decreased to about 10% of the injected dose at 30 min postinjection. In contrast, $(M6P)_{20}$-BSA-^{33}P-TFO was rapidly cleared from the circulation with only 15 and 5% of radioactivity detected in the plasma at 5 and 30 min postinjection. There was a significant increase in the accumulation of radioactivity in the liver. In the case of ^{33}P-TFO, almost 25% of the injected dose was detected in the plasma at 5 min but increased to 47% at 30 min postinjection. In the case of $(M6P)_{20}$-BSA-^{33}P-TFO, about 50% of the injected dose was detected in the liver at 5 min postinjection but increased to 66% at 30 min postinjection. The amount of radioactivity accumulated in the spleen and urine at 30

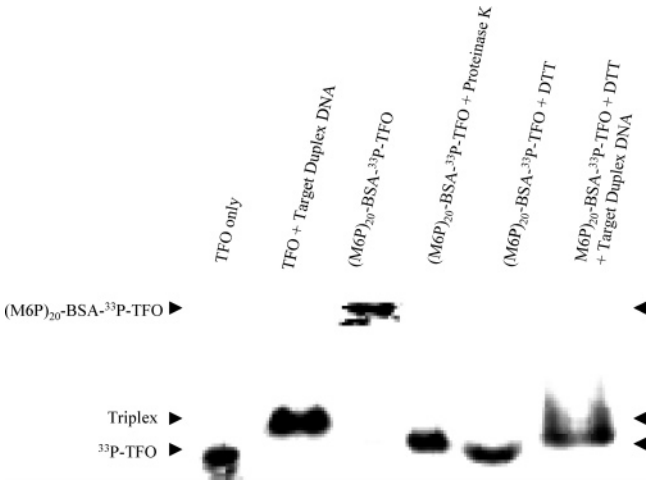

FIGURE 8: Triplex formation of TFO with duplex DNA. Samples were applied on 15% native PAGE at 4 °C in 89 mM Tris-borate buffer, containing $MgCl_2$ (20 mM) for 4 h. Lane 1: ^{33}P-TFO; lane 2: duplex DNA/^{33}P-TFO (1:500) incubated for 20 h at 37 °C; lane 3: $(M6P)_{20}$-BSA-^{33}P-TFO; lane 4: $(M6P)_{20}$-BSA-^{33}P-TFO incubated with Proteinase K for 2 h at 37 °C; lane 5: $(M6P)_{20}$-BSA-^{33}P-TFO incubated with DTT for 2 h at 37 °C; and lane 6: duplex DNA/$(M6P)_{20}$-BSA-^{33}P-TFO (molar ratio = 1:2) incubated for 6 h at 37 °C with DTT (0.2 M) treatment.

min postinjection was significantly higher than that at 5 min postinjection.

Hepatic Cellular Localization. To determine the uptake of $(M6P)_{20}$-BSA-^{33}P-TFO by different types of hepatic cells and to determine whether the uptake of $(M6P)_{20}$-BSA-^{33}P-TFO by HSCs is M6P/IGF II receptor-mediated, the liver was perfused at 30 min post tail vein injection of $(M6P)_{20}$-BSA-^{33}P-TFO and ^{33}P-TFO, and hepatocytes, Kupffer and endothelial cells, and HSCs were isolated for determination of the amount of radioactivity by these cells. As shown in Figure 10, TFO concentration in the HSCs was 1093 ng/mg cell protein at 30 min after intravenous injection of the $(M6P)_{20}$-BSA-^{33}P-TFO conjugate, but there was only 215 ng/mg cell protein in the case of ^{33}P-TFO. Accordingly, the uptake of $(M6P)_{20}$-BSA-^{33}P-TFO conjugate by hepatocytes and Kupffer and endothelial cells was higher than those of ^{33}P-TFO samples.

DISCUSSION

Excessive accumulation of type I and III collagens by HSCs is known to be the main cause of liver fibrosis. We have previously shown that 25mer antiparallel phosphorothioate (APS) TFO can form a triplex with the duplex DNA of the C_1 region (−170 to −141) of the α1 (I) procollagen gene promoter and effectively inhibit its transcription in vitro (*3*, *5*). Thus, the TFO against α1 (I) procollagen can be used as a potent antifibrotic drug. However, for the treatment of liver fibrosis, the problem lies in how the TFO can be delivered to the liver in general and more specifically to HSCs. In liver fibrosis, HSCs are activated, leading to the accumulation of a scar (fibril forming) matrix, which in turn contributes to the loss or narrowing of sinusoidal fenestrae (*30*, *31*). Therefore, TFO delivery to HSCs is expected to be much less in liver fibrotic rats and thus may not efficiently inhibit the production of the α1 (I) procollagen, considering that only a small fraction of free ODN could reach the target cell type and enter the cells.

We and others have shown that ODNs are cleared rapidly from the circulation and accumulated in most of the peripheral tissues, with the highest accumulation in the liver and kidney (*11*, *32*−*37*). To enhance a receptor-mediated ODN delivery to hepatocytes, we previously determined the

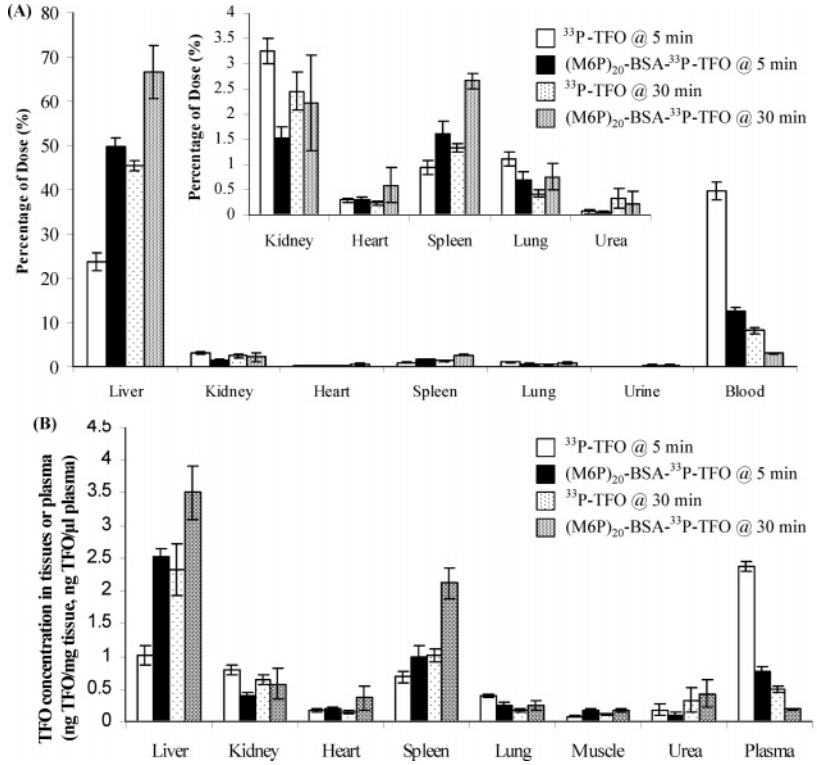

FIGURE 9: (A) Biodistribution of $(M6P)_{20}$-BSA-^{33}P-TFO and ^{33}P-TFO after intravenous injection into rats in percentage of injected dose (0.2 mg of TFO/kg of body weight). (B) TFO concentrations in different tissues and plasma. Values are expressed as means ± SD of four animals. ($p < 0.01$ when considering the differences in liver uptake between biodistributions of $(M6P)_{20}$-BSA-^{33}P-TFO and ^{33}P-TFO.)

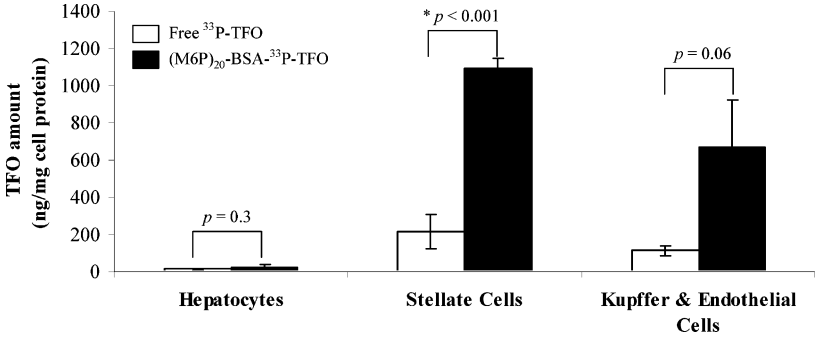

FIGURE 10: Uptake of $(M6P)_{20}$-BSA-^{33}P-TFO and ^{33}P-TFO by liver cell types. Rats were intravenously injected with ^{33}P-TFO (□) and $(M6P)_{20}$-BSA-^{33}P-TFO (■) at a dose of 0.2 mg of TFO/kg body weight. Total cell protein in each liver cell type was determined by BCA protein assay. The amount of TFO found in each cell type is given in ng per mg of cell protein. Values are means ± SD of three animals. *: statistically significant.

disposition characteristics of ^{35}S-ODNs and their galactosylated poly (L-lysine) (Gal-PLL) complexes in mice in relation to their physicochemical properties (*11*). Complex formation with Gal-PLL enhanced the hepatic uptake of ODNs. Although the uptake of PS ODNs/Gal-PLL complexes by hepatocytes was significantly higher than that of naked PS ODNs, the difference in their intracellular distribution was only moderate and dependent on the particle size, zeta potential. and number of galacotose residues. For asialoglycoprotein (ASGP) receptor-mediated uptake of ODNs by hepatocytes, Rajur et al. covalently conjugated ODNs to ASGP using sulfosuccinimidyl 6-[3′-(pyridyldithio)propionamido]hexanoate (Sulfo-LC-SPDP) (*38*).

M6P is a ligand for the M6P/IGF II receptor, which is expressed on the surface of the HSCs and is upregulated in activated HSCs (*15*, *39*). To avoid any nonspecific ionic interaction and the large particle size, in this study we conjugated TFOs to M6P-BSA via the disulfide bond for enhanced uptake by the HSCs. BSA is used to increase the circulation time of drug molecules, as BSA is neither phagocytosed by macrophages in the liver nor excreted by the kidney (*40*). There are sinusoidal gaps in the capillary endothelia of the liver, which allow passage of particles of less than 100 to ∼150 nm in size.

The use of M6P-BSA should enhance the hepatic uptake and reduce the renal clearance of the TFOs. Therefore, we synthesized $(M6P)_{20}$-BSA-^{33}P-TFO and determined their biodistribution in all major organs after systemic administration into rats. In the present study, we first synthesized $(M6P)_x$-BSA using varying ratios of itcM6P and BSA. TFO was attached to BSA via a disulfide bond, which is known to be stable in the circulation but cleaved intracellularly by thiols such as glutathione and/or redox enzymes or other mechanisms (*29*, *41*−*44*). Conjugation of $(M6P)_{20}$-BSA to the TFO was confirmed by electrophoresis on a polyacrylamide gel (Figure 6). Cleavage of the disulfide bond between BSA and TFO by DTT suggests that the linkage between M6P-BSA and TFO will also be cleaved easily inside cells. In the gel, there was also a band with a much higher molecular weight lying on the top of the gel, which was considered as the multimer of the M6P-BSA-^{33}P-TFO conjugate. This was confirmed by the fact of that when the conjugate was treated with Proteinase K (Figure 8, lane 4), this band disappeared. Proteinase K digested the BSA content in the conjugate and released the TFO as well. In addition, the $(M6P)_{20}$-BSA-^{33}P-TFO conjugate was very stable up to 6 h when incubated with the rat serum at 37 °C. There was no free isotope and no TFO molecules released, suggesting that the disulfide bonds will be cleaved only inside the target cells with reducing conditions.

A similar approach was also utilized by Bonfils et al., who conjugated antisense ODNs to M6P-BSA and showed enhanced uptake of M6P-BSA-ODN conjugates by macrophages and myofibroblast cell lines in vitro, but little uptake by U937 monocyte cells, which do not express M6P/IGF II receptors (*17*). In contrast, the uptake of free ODN was very low by all these cell lines. However, these authors did not evaluate M6P-BSA-ODN conjugates in vivo.

TFO can function well only when it can form a triplex with the genomic DNA in the nucleus of the target cells. However, by conjugation of molecules with TFO, the triplex formation property is often disturbed (*45*, *46*). This is not the case in our conjugation strategy since the carrier molecule will be cleaved before the TFO molecule reaches its target DNA. In our study, TFO was conjugated with the M6P-BSA via a disulfide bond so that the TFO can be released inside the cells. We determined whether the TFO could still form triplex with the duplex DNA of the C_1 region (−170 to approximately −141) of the α1 (I) collagen gene promoter when released from M6P-BSA. As shown in Figure 8, the released free TFO could form triplex with the target duplex DNA easily. Triplex formation between free TFO and the target duplex DNA was at the molar ratio of 500:1; in contrast, a portion of the released TFO from the conjugate formed the triplex even at the molar ratio of 2:1 (Figure 8). Since there is only one copy of the target genomic DNA sequence per HSC, TFO will be in much excess. Furthermore, we have shown previously that the increase in the molar ratio of TFO to DNA could enhance triplex formation (*5*).

Beljaars et al. have shown that $(M6P)_{21}$-BSA really gave enhanced uptake in HSCs in fibrotic rats, which was comparable to $(M6P)_{27}$-HSA. (*16*) In our study, we synthesized $(M6P)_{20}$-BSA-^{33}P-TFO, which contains 20 M6P residues per BSA for our biodistribution study. M6P-BSA conjugation to the TFO via disulfide bond significantly enhanced TFO delivery to the liver from 25% for ^{33}P-TFO to 50% for $(M6P)_{20}$-BSA-^{33}P-TFO at 5 min postinjection but increased from 47% (for ^{33}P-TFO) to 66% (for $(M6P)_{20}$-BSA-^{33}P-TFO) at 30 min postinjection.

The hepatic uptake of phosphorothioate ODN is known to be taken up mostly by endothelial cells (*32*, *47*, *48*).

Kupffer cells only contribute a little fraction, and hepatocytes are the least even though they are the most abundant cells in the liver. There is little information on the uptake of ODNs by HSCs since most of the studies did not separate the HSCs from endothelial cells and Kupffer cells. Conjugation with cholesterol has also been shown to enhance ODN delivery to the liver (*12*, *49*). These authors have shown that when conjugated with cholesterol, ODNs are mostly taken up by Kupffer cells instead of endothelial cells in the liver.

To determine the hepatic cellular localization, we perfused the liver at 30 min postinjection of $(M6P)_{20}$-BSA-^{33}P-TFO and separated different liver cells by fractionation on the Nycodenz gradient. As shown in Figure 10, the TFO concentration in the HSCs was 1093 ng/mg cell protein when $(M6P)_{20}$-BSA-^{33}P-TFO was injected into rats as compared to only 215 ng/mg cell protein for ^{33}P-TFO injected samples. There was also increase in the TFO concentration (from 112 to 670 ng/mg cell protein) in the mixture of the Kupffer and endothelial cells for $(M6P)_{20}$-BSA-^{33}P-TFO. The TFO concentration in the hepatocytes was very low in both cases. The surprising finding was that HSCs contribute more than Kupffer and endothelial cells in the total liver uptake of TFOs.

Graham et al. (*33*) had reported that a large proportion (~80% of the ODNs in the liver) of the injected PS ODNs was taken up by the Kupffer and endothelial cells. The remaining 20% was taken up by the hepatocytes. Bijsterbosch et al. also reported that almost 70% of the liver recovery was associated with nonparenchymal cells such as endothelial and Kupffer cells (*12*). However, these authors did not isolate HSCs; thus, the reported uptake of PS ODNs by Kupffer and endothelial cells is overestimated since HSCs are likely to be present in the Kupffer and endothelial cell preparations. Since HSCs are the key fibrogenic cells, which are responsible for the synthesis of ECM components, it is important to know the uptake of TFOs by these cells.

In the present study, we isolated Kupffer, endothelial, and HSCs by fractionation on Nycodenz gradient as described by Hendriks et al. (*25*). Moreover, we ensured the purity of isolated HSCs by autofluoroscence and staining with desmin antibodies (K. Cheng et al., manuscript in preparation). To our knowledge, this is the first report on TFO delivery to HSCs. Even though the TFO itself was also primarily taken up by HSCs, the total recovery of TFO molecules in these cells was much lower than that of the conjugate. Since the uptake of $(M6P)_{20}$-BSA-^{33}P-TFO is likely to be dependent on the number of M6P residues per BSA, more experiments will be done to optimize the number of M6P residues per BSA conjugate for efficient TFO delivery to HSCs of both normal and fibrotic rats. Our delivery system is potentially more useful for the treatment of liver fibrosis by concentrating TFO molecules in HSCs at low doses. TFOs are not only expensive but also have the potential to be toxic at very high doses.

In conclusion, we have synthesized M6P-BSA and conjugated it to TFO via a disulfide bond, which was stable in rat serum but could be cleaved in the presence of reducing reagents. Moreover, we have shown enhanced delivery of $(M6P)_{20}$-BSA-^{33}P-TFO to the liver and the increased TFO concentration in the HSCs as compared with ^{33}P-TFO. Therefore, we believe our TFO against the α1 (I) collagen gene promoter can be used for the treatment of liver fibrosis. We are currently evaluating the effect of the number of M6P per BSA molecules on the TFO delivery to the liver in general and HSCs in particular. Since the TFO has to enter the nucleus for triplex formation with the α1 (I) collagen gene promoter, studies are underway to determine the subcellular distribution of M6P-BSA-^{33}P-TFO in the cytoplasm and nuclear extracts after intravenous injection of M6P-BSA-^{33}P-TFO. Then, we will determine its effect on collagen gene expression by hydroxyproline assay of the liver extracts with a fibrotic rat model.

REFERENCES

1. Raghow, R. (1994) The role of extracellular matrix in postinflammatory wound healing and fibrosis, *FASEB J. 8*, 823−31.
2. Knittel, T., Schuppan, D., Meyer zum Buschenfelde, K. H., and Ramadori, G. (1992) Differential expression of collagen types I, III, and IV by fat-storing (Ito) cells in vitro, *Gastroenterology 102*, 1724−35.
3. Nakanishi, M., Weber, K. T., and Guntaka, R. V. (1998) Triple helix formation with the promoter of human alpha 1(I) procollagen gene by an antiparallel triplex-forming oligodeoxyribonucleotide, *Nucleic Acids Res. 26*, 5218−22.
4. Kovacs, A., Kandala, J. C., Weber, K. T., and Guntaka, R. V. (1996) Triple helix-forming oligonucleotide corresponding to the polypyrimidine sequence in the rat alpha 1(I) collagen promoter specifically inhibits factor binding and transcription, *J. Biol. Chem. 271*, 1805−12.
5. Joseph, J., Kandala, J. C., Veerapanane, D., Weber, K. T., and Guntaka, R. V. (1997) Antiparallel polypurine phosphorothioate oligonucleotides form stable triplexes with the rat alpha 1(I) collagen gene promoter and inhibit transcription in cultured rat fibroblasts, *Nucleic Acids Res. 25*, 2182−8.
6. Bataller, R., and Brenner, D. A. (2001) Hepatic stellate cells as a target for the treatment of liver fibrosis, *Semin. Liver Dis. 21*, 437−51.
7. Reeves, H. L., and Friedman, S. L. (2002) Activation of hepatic stellate cells—a key issue in liver fibrosis, *Frontiers Biosci. 7*, d808−26.
8. Sawai, K., Mahato, R. I., Oka, Y., Takakura, Y., and Hashida, M. (1996) Disposition of oligonucleotides in isolated perfused rat kidney: involvement of scavenger receptors in their renal uptake, *J. Pharmacol. Exp. Ther. 279*, 284−90.
9. Yoshida, M., Mahato, R. I., Kawabata, K., Takakura, Y., and Hashida, M. (1996) Disposition characteristics of plasmid DNA in the single-pass rat liver perfusion system, *Pharm. Res. 13*, 599−603.
10. Takakura, Y., Mahato, R. I., Yoshida, M., Kanamaru, T., and Hashida, M. (1996) Uptake characteristics of oligonucleotides in the isolated rat liver perfusion system, *Antisense Nucleic Acid Drug Dev. 6*, 177−83.
11. Mahato, R. I., Takemura, S., Akamatsu, K., Nishikawa, M., Takakura, Y., and Hashida, M. (1997) Physicochemical and disposition characteristics of antisense oligonucleotides complexed with glycosylated poly(L-lysine), *Biochem. Pharmacol. 53*, 887−95.
12. Bijsterbosch, M. K., Manoharan, M., Dorland, R., Waarlo, I. H., Biessen, E. A., and van Berkel, T. J. (2001) Delivery of cholesteryl-conjugated phosphorothioate oligodeoxynucleotides to Kupffer cells by lactosylated low-density lipoprotein, *Biochem. Pharmacol. 62*, 627−33.
13. Geerts, A. (2001) History, heterogeneity, developmental biology, and functions of quiescent hepatic stellate cells, *Semin. Liver Dis. 21*, 311−35.
14. de Bleser, P. J., Jannes, P., van Buul-Offers, S. C., Hoogerbrugge, C. M., van Schravendijk, C. F., Niki, T., Rogiers, V., van den Brande, J. L., Wisse, E., and Geerts, A. (1995) Insulinlike growth factor-II/mannose 6-phosphate receptor is expressed on CCl4-exposed rat fat-storing cells and facilitates activation of latent transforming growth factor beta in cocultures with sinusoidal endothelial cells, *Hepatology 21*, 1429−37.
15. Weiner, J. A., Chen, A., and Davis, B. H. (1998) E-box-binding repressor is down-regulated in hepatic stellate cells during up-regulation of mannose 6-phosphate/insulin-like growth factor-II receptor expression in early hepatic fibrogenesis, *J. Biol. Chem. 273*, 15913−9.

16. Beljaars, L., Molema, G., Weert, B., Bonnema, H., Olinga, P., Groothuis, G. M., Meijer, D. K., and Poelstra, K. (1999) Albumin modified with mannose 6-phosphate: A potential carrier for selective delivery of antifibrotic drugs to rat and human hepatic stellate cells, *Hepatology 29*, 1486−93.
17. Bonfils, E., Depierreux, C., Midoux, P., Thuong, N. T., Monsigny, M., and Roche, A. C. (1992) Drug targeting: synthesis and endocytosis of oligonucleotide−neoglycoprotein conjugates, *Nucleic Acids Res. 20*, 4621−9.
18. Roche, A. C., Midoux, P., Bouchard, P., and Monsigny, M. (1985) Membrane lectins on human monocytes. Maturation-dependent modulation of 6-phosphomannose and mannose receptors, *FEBS Lett. 193*, 63−8.
19. Monsigny, M., Roche, A. C., and Midoux, P. (1984) Uptake of neoglycoproteins via membrane lectin(s) of L1210 cells evidenced by quantitative flow cytofluorometry and drug targeting, *Biol. Cell 51*, 187−96.
20. Sando, G. N., and Karson, E. M. (1980) *p*-Isothiocyanatophenyl 6-phospho-_-D-mannopyranoside coupled to albumin. A model compound recognized by the fibroblast lysosomal enzyme uptake system. 1. Chemical synthesis and characterization, *Biochemistry 19*, 3850−5.
21. Breton, P., Midoux, P., Petit, C., Bousser, M. T., Roche, A. C., Mayer, R., and Monsigny, M. (1991) Production of macrophage-derived cytotoxic factor by *N*-[3-[(carbamoylmethyl)thio]propionylated] neoglycoproteins, *Bioconjug. Chem. 2*, 16−8.
22. Carlsson, J., Drevin, H., and Axen, R. (1978) Protein thiolation and reversible protein−protein conjugation. *N*-Succinimidyl 3-(2-pyridyldithio)propionate, a new heterobifunctional reagent, *Biochem. J. 173*, 723−37.
23. Monsigny, M., Petit, C., and Roche, A. C. (1988) Colorimetric determination of neutral sugars by a resorcinol sulfuric acid micromethod, *Anal. Biochem. 175*, 525−30.
24. Blomhoff, R., and Berg, T. (1990) Isolation and cultivation of rat liver stellate cells, *Methods Enzymol. 190*, 58−71.
25. Hendriks, H. F., Brouwer, A., and Knook, D. L. (1990) Isolation, purification, and characterization of liver cell types, *Methods Enzymol. 190*, 49−58.
26. Nagelkerke, J. F., Barto, K. P., and van Berkel, T. J. (1983) In vivo and in vitro uptake and degradation of acetylated low-density lipoprotein by rat liver endothelial, Kupffer, and parenchymal cells, *J. Biol. Chem. 258*, 12221−7.
27. Zhang, J., Zhang, Q. S., Chen, X. M., and Tian, G. Y. (2002) Synthesis of a targeting drug for antifibrosis of liver; a conjugate for delivering glycyrrhetin to hepatic stellate cells, *Glycoconj. J. 19*, 423−9.
28. Poon, K., and Macgregor, R. B., Jr. (1998) Unusual behavior exhibited by multistranded guanine-rich DNA complexes, *Biopolymers 45*, 427−34.
29. Wang, L., Kristensen, J., and Ruffner, D. E. (1998) Delivery of antisense oligonucleotides using HPMA polymer: synthesis of A thiol polymer and its conjugation to water-soluble molecules, *Bioconjug. Chem. 9*, 749−57.
30. Safadi, R., and Friedman, S. L. (2002) Hepatic fibrosis−role of hepatic stellate cell activation, *MedGenMed 4*, 27.
31. Friedman, S. L. (2000) Molecular regulation of hepatic fibrosis, an integrated cellular response to tissue injury, *J. Biol. Chem. 275*, 2247−50.
32. Graham, M. J., Crooke, S. T., Lemonidis, K. M., Gaus, H. J., Templin, M. V., and Crooke, R. M. (2001) Hepatic distribution of a phosphorothioate oligodeoxynucleotide within rodents following intravenous administration, *Biochem. Pharmacol. 62*, 297−306.
33. Graham, M. J., Crooke, S. T., Monteith, D. K., Cooper, S. R., Lemonidis, K. M., Stecker, K. K., Martin, M. J., and Crooke, R. M. (1998) In vivo distribution and metabolism of a phosphorothioate oligonucleotide within rat liver after intravenous administration, *J. Pharmacol. Exp. Ther. 286*, 447−58.
34. Rusckowski, M., Qu, T., Roskey, A., and Agrawal, S. (2000) Biodistribution and metabolism of a mixed backbone oligonucleotide (GEM 231) following single and multiple dose administration in mice, *Antisense Nucleic Acid Drug Dev. 10*, 333−45.
35. Agrawal, S., Tan, W., Cai, Q., Xie, X., and Zhang, R. (1997) In vivo pharmacokinetics of phosphorothioate oligonucleotides containing contiguous guanosines, *Antisense Nucleic Acid Drug Dev. 7*, 245−9.
36. Temsamani, J., Roskey, A., Chaix, C., and Agrawal, S. (1997) In vivo metabolic profile of a phosphorothioate oligodeoxyribonucleotide, *Antisense Nucleic Acid Drug Dev. 7*, 159−65.
37. Grindel, J. M., Musick, T. J., Jiang, Z., Roskey, A., and Agrawal, S. (1998) Pharmacokinetics and metabolism of an oligodeoxynucleotide phosphorothioate (GEM91) in cynomolgus monkeys following intravenous infusion, *Antisense Nucleic Acid Drug Dev. 8*, 43−52.
38. Rajur, S. B., Roth, C. M., Morgan, J. R., and Yarmush, M. L. (1997) Covalent protein-oligonucleotide conjugates for efficient delivery of antisense molecules, *Bioconjug. Chem. 8*, 935−40.
39. Weiner, J. A., Chen, A., and Davis, B. H. (2000) Platelet-derived growth factor is a principal inductive factormodulating mannose 6-phosphate/insulin-like growth factor-II receptorgene expression via a distal E-box in activated hepatic stellate cells, *Biochem. J. 345* Pt 2, 225−31.
40. Shinoda, T., Takagi, A., Maeda, A., Kagatani, S., Konno, Y., and Hashida, M. (1998) In vivo fate of folate-BSA in nontumor- and tumor-bearing mice, *J. Pharm. Sci. 87*, 1521−6.
41. Shen, W. C., Ryser, H. J., and LaManna, L. (1985) Disulfide spacer between methotrexate and poly(d-lysine). A probe for exploring the reductive process in endocytosis, *J. Biol. Chem. 260*, 10905−8.
42. Feener, E. P., Shen, W. C., and Ryser, H. J. (1990) Cleavage of disulfide bonds in endocytosed macromolecules. A process not associated with lysosomes or endosomes, *J. Biol. Chem. 265*, 18780−5.
43. Kang, Y. S., Voigt, K., and Bickel, U. (2000) Stability of the disulfide bond in an avidin−biotin linked chimeric peptide during in vivo transcytosis through brain endothelial cells, *J. Drug Target 8*, 425−34.
44. Kwok, K. Y., Park, Y., Yang, Y., McKenzie, D. L., Liu, Y., and Rice, K. G. (2003) In vivo gene transfer using sulfhydryl cross-linked PEG-peptide/glycopeptide DNA cocondensates, *J. Pharm. Sci. 92*, 1174−85.
45. Rapozzi, V., Cogoi, S., Spessotto, P., Risso, A., Bonora, G. M., Quadrifoglio, F., and Xodo, L. E. (2002) Antigene effect in K562 cells of a PEG-conjugated triplex-forming oligonucleotide targeted to the bcr/abl oncogene, *Biochemistry 41*, 502−10.
46. Zhilina, Z. V., Ziemba, A. J., Trent, J. O., Reed, M. W., Gorn, V., Zhou, Q., Duan, W., Hurley, L., and Ebbinghaus, S. W. (2004) Synthesis and evaluation of a triplex-forming oligonucleotide−pyrrolobenzodiazepine conjugate, *Bioconjug. Chem. 15*, 1182−92.
47. Biessen, E. A., Vietsch, H., Kuiper, J., Bijsterbosch, M. K., and Berkel, T. J. (1998) Liver uptake of phosphodiester oligodeoxynucleotides is mediated by scavenger receptors, *Mol. Pharmacol. 53*, 262−9.
48. Bijsterbosch, M. K., Manoharan, M., Rump, E. T., De Vrueh, R. L., van Veghel, R., Tivel, K. L., Biessen, E. A., Bennett, C. F., Cook, P. D., and van Berkel, T. J. (1997) In vivo fate of phosphorothioate antisense oligodeoxynucleotides: predominant uptake by scavenger receptors on endothelial liver cells, *Nucleic Acids Res. 25*, 3290−6.
49. Bijsterbosch, M. K., Manoharan, M., Dorland, R., Van Veghel, R., Biessen, E. A., and Van Berkel, T. J. (2002) bis-Cholesteryl-conjugated phosphorothioate oligodeoxynucleotides are highly selectively taken up by the liver, *J. Pharmacol. Exp. Ther. 302*, 619−26.

BI047529J